Parametric Investigation of the Deflection Performance of Serial Piezoelectric C-Block Actuators

ANDREW J. MOSKALIK AND DIANN BREI*
Department of Mechanical Engineering and Applied Mechanics, The University of Michigan, 2250 G. G. Brown Building, Ann Arbor, MI 48109-2125

ABSTRACT: This paper presents an investigation of the deflection performance of serial configurations of C-block piezoelectric actuators. To conduct the investigation both a theoretical and an experimental approach were used. A theoretical model was derived and experimentally verified with six different case studies. These experimental case studies were used to explore the effect on the deflection performance by modifying the geometric, material, and configuration parameters. The results demonstrate the wide versatility possible with serial C-block actuation architectures.

INTRODUCTION

PIEZOELECTRIC actuators are often used in many intelligent structure applications such as active rotor blade flaps and space trusses that are space- or weight-constrained because these actuators are small and light and consume little power (Damjanovic and Newnham, 1992). Most piezoelectric actuators employed fall into one of two categories: stacks (Spencer and Chopra, 1996), that produce high forces and small deflections, and benders, straight or tapered (Ben-Zeev and Chopra, 1996; Hall and Prechtl, 1996), that generate large deflection and small forces. To use stacks that generate deflections large enough for many applications, a common approach is to construct mechanical leveraging systems to improve deflection performance at the expense of force generation capability (Bamford et al., 1995; Samak and Chopra, 1996). However, this approach frequently suffers from transmission losses (Paine and Chaudhry, 1996) and may create difficulties in packaging the additional external leveraging mechanisms. On the other hand, bender actuators are internally leveraged, producing greater deflections than stacks, and thus do not require external leveraging. Unfortunately, the greater output deflection obtained by using benders comes at a significant cost in output force. Recently, there have been a number of novel piezoelectric actuator architectures invented that utilize external amplification schemes, such as cymbals (Dogan, Uchino, and Newnham, 1997) and moonies (Onitsuka et al., 1995), and internal amplification schemes such as RAINBOW actuators (Haertling, 1994), CRESCENT actuators (Chandran, Kugel, and Cross, 1997) and THUNDER actuators (Face International, 1997). Unfortunately, according to Kugel, Chandran and Cross (1997), all of these architectures are less efficient than the straight bender.

An alternative approach that is currently being investigated is internally leveraged actuators called C-blocks. Individual C-blocks are constructed from semicircular piezoelectric material poled in the radial direction and activated in the circumferential direction by a voltage applied across the thickness, causing the entire architecture to flex (Brei, Ervin, and Moskalik, 1997; Moskalik and Brei, 1996, 1997a, 1997b). Research on individual C-blocks has demonstrated that C-blocks can generate 2.67 times the force of a straight bender with 40.5% of the deflection, thus producing 8% more work than a straight bender constructed from the same volume of piezoelectric material (Moskalik and Brei, 1996, 1997b). To compensate for the loss of deflection, individual C-blocks can be combined in series to increase the total output deflection [Figure 1(a)]. In serial C-blocks, each individual C-block is oriented such that the output deflections add [Figure 1(b)].

The main advantage to this serial type of actuator architecture is the diverse number of configurations and performance characteristics that can be achieved by altering the geometric and material parameters and the number of C-blocks in the series. This is helpful when trying to meet challenging performance characteristics while fitting the actuator within different application volumes. Of course altering the geometric parameters of the C-block alters the volumetric packaging efficiency of the C-block series and C-blocks cannot be packed as tightly as straight bender architectures in rectangular application spaces.

However, being able to combine C-blocks in series provides an additional design parameter that is not available in many other actuation architectures such as straight benders. With this additional design parameter, more actuation options are available for a given set of requirements. This parameter, therefore, is very useful due to the increase in feasible options available. This can be critical when designing an actuator to meet challenging application performance requirements while at the same time having to meet strict package constraints or odd shapes.

*Author to whom correspondence should be addressed.

1045-389X/98/03 0223-09 $10.00/0

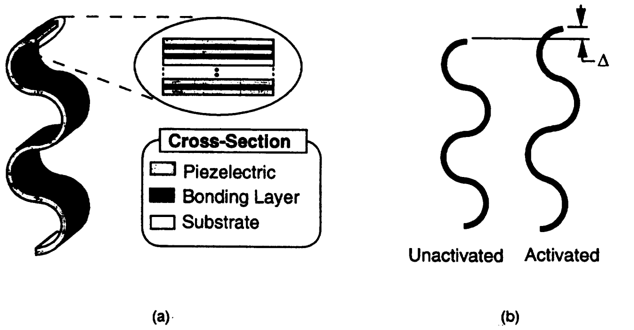

Figure 1. Piezoceramic C-block serial actuator design and operation. (a) Serial C-block actuators can be constructed by joining individual C-blocks. (b) The serial C-block produces a deflection, Δ, at the tip of the series.

While the individual C-block has already been characterized (Brei, Ervin, and Moskalik, 1997; Moskalik and Brei, 1996, 1997a, 1997b), the examination of the serial C-block configurations is just beginning. This paper presents an in-depth investigation of the deflection response of serial C-block actuation architectures. It includes the derivation of a simple but useful model to predict the deflection-voltage behavior of a generic serial C-block actuator. In addition, results are given from an extensive experimental study which was conducted to validate the theoretical models and to explore the versatility of the serial architectures through changes in the geometric, material, and configuration design parameters.

THEORETICAL INVESTIGATION

To investigate the deflection capabilities of serial C-block architectures, a theoretical model for the deflection-voltage performance was derived by determining the strain energy stored in an individual C-block, summing the energy for all C-blocks in the series, and applying Castigliano's theorem to derive the deflection-voltage model. During the derivation, the C-block was assumed to be a thin, perfectly bonded laminate curved beam with q layers, including piezoelectric, bonding, electrode, and substrate layers. Each individual C-block was assumed identical. The nomenclature used is shown in Figure 2, where Δ is the tip deflection, R_n is the neutral axis radius, b is width, and z is distance from the neutral axis to the outside of a layer, and F_Δ is a virtual load applied at the C-block tip in the direction of the tip deflection.

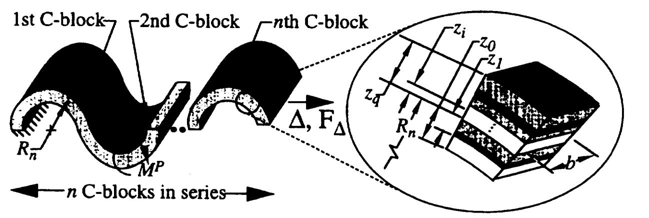

Figure 2. Nomenclature used in theoretical model derivation. The serial C-block is made up of n individual C-blocks, each with a neutral axis of R_n and identical cross-section. The total tip deflection is Δ, F_Δ is a virtual force, z is the distance to the outside of a layer, and b is the layer width.

The complementary strain energy, U^*, contained in each individual C-block making up the series is a function of the internal moment within the C-block. The internal moment is the sum of the piezoelectric moment, M^P, and the moment induced by the virtual load, F_Δ.

$$M = M^P + F_\Delta R_n \sin\theta \tag{1}$$

The strain energy within one C-block can be derived by squaring the internal moment [Equation (1)], dividing by the composite bending stiffness, D, and integrating along the length of the C-block,

$$U^* = \int_0^\pi \frac{(M^P + F_\Delta R_n \sin\theta)^2}{2D} R_n d\theta \tag{2}$$

The piezoelectric moment, M^P, and composite bending stiffness, D, are calculated by integrating across the cross-sectional area of a generic C-block of q layers (Moskalik and Brei, 1997a, 1997b), and are defined as

$$M^P = \sum_{i=1}^{q} \frac{1}{2} Y_i b_i (d_{31}V)_i (z_i + z_{i-1}) \tag{3}$$

and

$$D = \sum_{i=1}^{q} \frac{1}{3} Y_i b_i (z_i^3 - z_{i-1}^3) \tag{4}$$

where Y is the Young's modulus, d_{31} is the piezoelectric constant, V is the applied voltage, and the subscript i refers to the ith layer. The C-block is assumed thin enough that the electric field within the ith layer is the voltage, V, divided by the thickness, $(z_i - z_{i-1})$. Since each individual C-block is identical, the total strain energy contained in the series is the number of C-blocks in series, n, multiplied by the energy within one C-block [Equation (2)],

$$U^*_{total} = n\int_0^\pi \frac{(M^P + F_\Delta R_n \sin\theta)}{2D} R_n d\theta \tag{5}$$

Castigliano's second theorem states that the deflection, Δ, is found by taking the partial derivative of the total complementary strain energy contained within all C-blocks with respect to a virtual load, F_Δ, applied in the direction of displacement. Differentiating the total strain energy [Equation (5)] results in,

$$\Delta = \frac{\partial U^*_{total}}{\partial F_\Delta} = n\int_0^\pi \frac{M^P R_n^2}{D} \sin\theta d\theta \tag{6}$$

where the virtual load, F_Δ, has been set to zero to produce the free deflection.

Performing the integration in Equation (6) results in a deflection-voltage model of

$$\Delta = \frac{2nM^P R_n^2}{D} \tag{7}$$

where this simple model relates the tip deflection, Δ, to the number of C-blocks in series, n, and the parameters of radius, R_n, bending stiffness, D, and internal moment, M^P, of the C-block series. Substituting in the expressions for moment and bending stiffness for a generic cross-section, the model can be explicitly written in terms of geometric parameters, material parameters, and applied voltage, V,

$$\Delta = \frac{3nR_n^2 \sum_{i=1}^{q} Y_i b_i (d_{31}V)_i (z_i + z_{i-1})}{\sum_{i=1}^{q} Y_i b_i (z_i^3 - z_{i-1}^3)} \tag{8}$$

This relationship states that both the voltage, V, and serial configuration parameter, n, are directly proportional to the deflection, resulting in a linear relationship. This straightforward relationship between the deflection and the serial configuration parameter makes it easy to tailor the actuator for a set of requirements because the total deflection of the serial actuator is simply the linear addition of the deflections of the individual C-blocks comprising the actuator. The relationship between deflection and the material and geometric parameters is more complicated. However, because the serial configuration, material, and geometric parameters are independent, it is possible to manipulate them to design a family of actuators with a wide deflection performance range, or to design a family of actuators with the same deflection performance but a very different volumetric package.

EXPERIMENTAL STUDIES

To confirm the deflection-voltage model and investigate the versatility of serial C-block actuators, an experimental investigation was conducted employing six case studies (Figure 3).

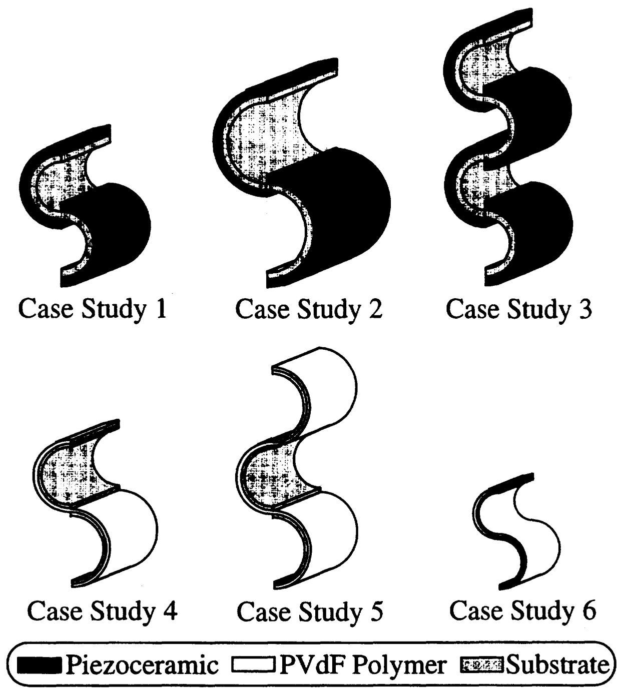

Figure 3. *Experimental case studies. Prototypes for six experimental case studies were fabricated. The first, baseline case study was comprised of a series of two piezoceramic C-blocks. The second case study was comprised of two piezoceramic C-blocks of larger radius; the third case study was comprised of a series of four C-blocks with the same radius as the first case study. The fourth and fifth case studies were comprised of series of two and three PVdF C-blocks, respectively; the sixth case study was comprised of a series of two PVdF C-blocks with two layers of piezoelectric material.*

- Case Study 1: Series of Two PZT-5H C-blocks. A baseline case study was undertaken to confirm the theoretical model and to use as a point of reference to compare to results from subsequent case studies. This case study consisted of a series of two unimorph C-blocks fabricated from one layer of PZT-5H piezoceramic material bonded to a substrate.
- Case Study 2: Series of Two PZT-8 C-blocks. A second case study, consisting of a series of two unimorph PZT-8 C-blocks of larger radius and thinner cross-section, was undertaken to determine the effect of geometric changes. The ability to change different geometric parameters to increase deflection expands the design versatility of the C-block series when it is used for space-constrained applications.
- Case Study 3: Series of Four PZT-5H C-blocks. The third case study, consisting of a series of four unimorph PZT-5H C-blocks of the same radius as the baseline, was undertaken to determine the effect of additional C-blocks. The simplicity of adding of C-blocks in series to linearly increase deflection is a major advantage of C-blocks over conventional straight benders.
- Case Study 4: Series of Two PVdF C-blocks. The fourth case study, consisting of a series of two unimorph Polyvinylidene Fluoride (PVdF) C-blocks, was undertaken to determine the effect of using a very different piezoelectric material, a polymeric, rather than piezoceramic material. The polymeric materials are substantially more compliant than the piezoceramic materials used in the first three case studies, and therefore this case study broadens the range of deflection performance investigated.
- Case Study 5: Series of Three PVdF C-blocks. The fifth case study, consisting of a series of three unimorph PVdF C-blocks of nearly the same radius as the fourth case study, was undertaken to determine the performance of a series containing an odd number of C-blocks.

- Case Study 6: Series of Two PVdF C-blocks. The sixth case study, consisting of a series of two bimorph PVdF C-blocks containing two piezoelectric layers, was undertaken to determine the effect of a cross-section containing more than one piezoelectric layer as is commonly done with other conventional actuators.

These case studies spanned a wide range of volumetric package sizes with heights ranging from about 8 mm to about 32 mm and lengths ranging from about 16 mm to about 67 mm. All six case studies were used to verify the accuracy of the theoretical model derived and the effect of changes in design parameters on the deflection performance.

Prototype Fabrication

Fabrication methods were developed for both piezoceramic and polymeric materials. Due to the differences in these materials, two different methods were utilized to construct prototypes.

PIEZOCERAMIC

Piezoceramic prototypes for the first three case studies were fabricated from circular piezoceramic tubes, either of PZT-5H or of PZT-8, manufactured by Morgan Matroc Electro Ceramics Division. The inner and outer radii of the tubes were pre-plated with a silver electrode a few microns thick. To fabricate the piezoceramic actuator, each tube was placed in a fixture, shown in Figure 4(a), and cut into two semicircular sections [Figure 4(b)] using a diamond saw. A steel strip was formed into an S-shape, shown in Figure 4(c), to conform to the inner diameter of the piezoceramic tubes, with loops in the steel equal to the number of C-blocks in the final prototype. This steel strip formed the backbone of the C-block actuator. The piezoceramic material was epoxied to the steel with an Insulcast 501 epoxy manufactured by Per-

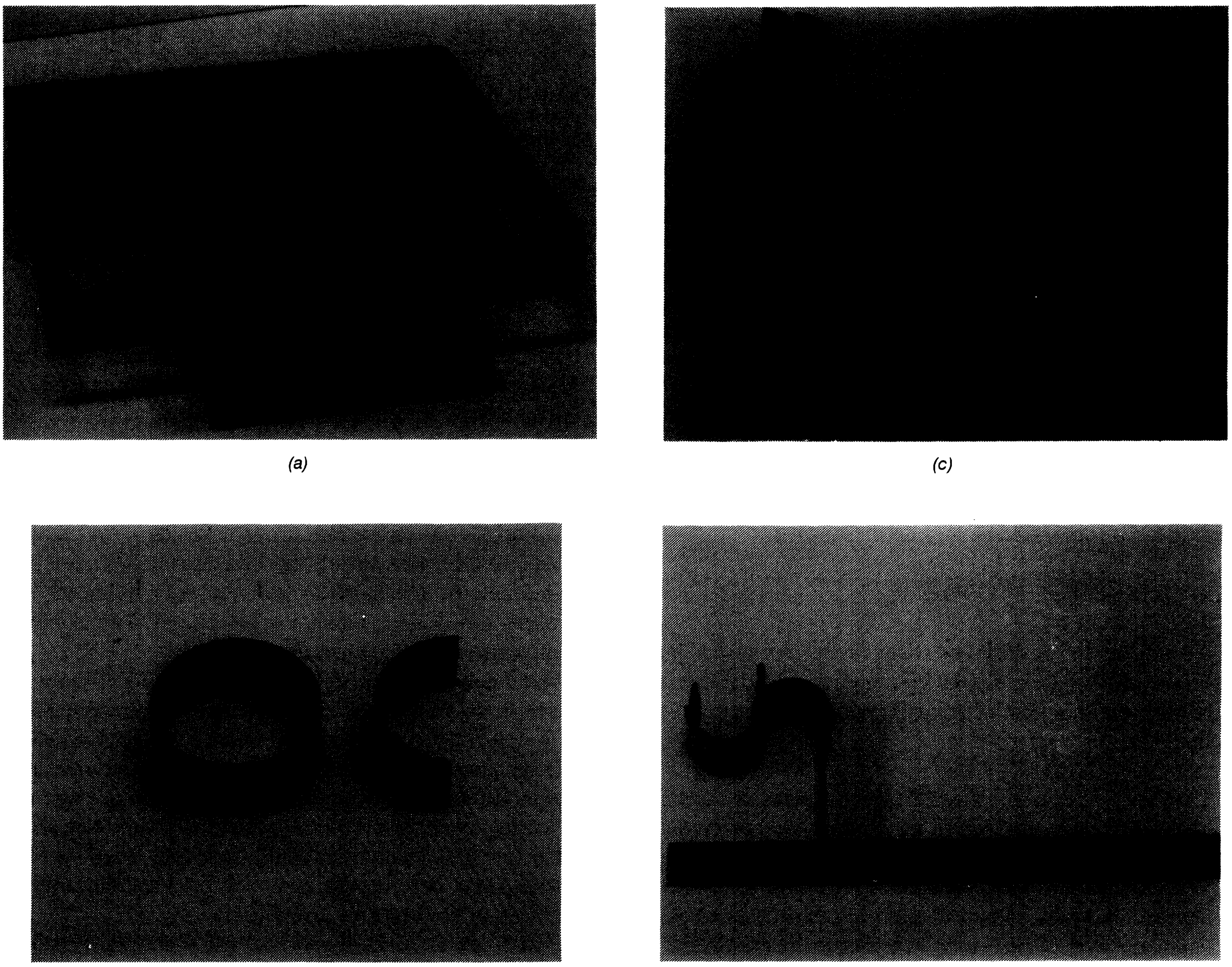

(a) (c) (b) (d)

Figure 4. *Fabrication of piezoceramic serial C-block actuators. The piezoceramic serial C-block actuators were fabricated from tubes of PZT-5H or PZT-8 piezoceramic. (a) These tubes were placed in a fixture and (b) sectioned into semicircles using a diamond saw. (c) The resulting piezoceramic semicircles were bonded to a steel substrate. (d) After curing, electrode wires were soldered on to form the finished prototype.*

Table 1. Geometric parameters for prototypes.

Case Study	Prototype Description	Outer Radius, R_{out} (mm)	Piezoelectric Thickness, t_p (mm)	Substrate Thickness, t_s (mm)	Total Thickness (mm)
1	(2) PZT-5H C-blocks	9.5	1.00	0.71	1.89
2	(2) PZT-8 C-blocks	15.9	0.76	0.41	1.30
3	(4) PZT-5H C-blocks	9.5	1.00	0.46	1.64
4	(2) PVdF C-blocks	11.0	0.052	0.025	0.139
5	(3) PVdF C-blocks	10.8	0.052	0.025	0.139
6	(2) PVdF C-blocks	3.95	0.052	none	0.155

Dimensions of the individual C-blocks comprising the serial prototypes used in the six case studies.

magile Industries. After the epoxy had cured, the individual piezoceramics were jumpered together to form the final prototype, shown in Figure 4(d). Prototypes for the three piezoceramic case studies were fabricated using this process and the parameters for all three piezoceramic prototypes are given in Table 1.

POLYMERIC

Prototypes for the polymeric case studies were fabricated from PVdF film manufactured by AMP Incorporated. The film was pre-electroded with a silver electrode and covered with a protective coating. To fabricate the piezoceramic actuators for case studies four and five, each film was epoxied to alternating aluminum substrates using an Insulcast 501 epoxy manufactured by Permagile Industries. For the sixth case study, two layers of polymeric film were etched with a special electrode pattern (Brei and Moskalik, 1997) to alternate the polarity of the field between adjacent C-blocks. The etched films were then bonded together with Insulcast 501 epoxy. For all three prototypes, the bonded film was wrapped around dowels in alternating directions as shown in Figure 5(a) and the epoxy was allowed to cure. The film was then removed from the dowels and electrodes were attached to form the final prototypes, shown in Figure 5(b). Parameters for the polymeric prototypes are given in Table 1.

Experimental Procedure

All of the prototypes were tested in the experimental setup shown in Figure 6. To perform the deflection-voltage experimental testing, each prototype was securely clamped in a vise and connected to an Oregon Electronics Model D4 DC voltage supply which was monitored with a Fluke multimeter. For the piezoceramic case studies and the last polymeric case study, the deflection of the C-block tip was measured using a Philtec A88NE1 fiber optic displacement sensor, and read using another Fluke multimeter. For the fourth and fifth case studies using polymeric prototypes, the deflection of the C-block tip was beyond the range of the fiber optic displacement sensor, and thus the displacement was measured using an MTI Microtrak 7000 laser displacement sensor.

The same procedure was used to determine the deflection-voltage performance for all the case studies. For each case study, the input DC voltage was incremented from zero volts to a maximum in regular intervals. At each interval, the deflection of the tip of the C-block was measured us-

(a)

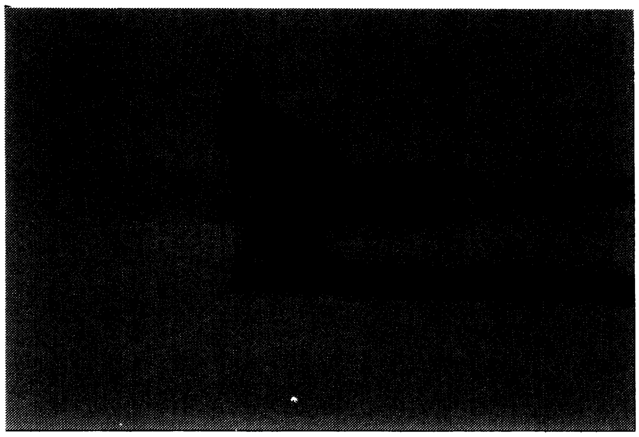

(b)

***Figure 5.** Fabrication of polymeric PVdF serial C-block actuators. The polymeric serial C-block actuators were fabricated from PVdF piezoelectric film. (a) The PVdF film was bonded to aluminum foil or to another layer of film and wrapped around a dowel fixture. (b) After the epoxy cured, the prototypes were clamped between glass slides and connected to electrodes to form the final prototype.*

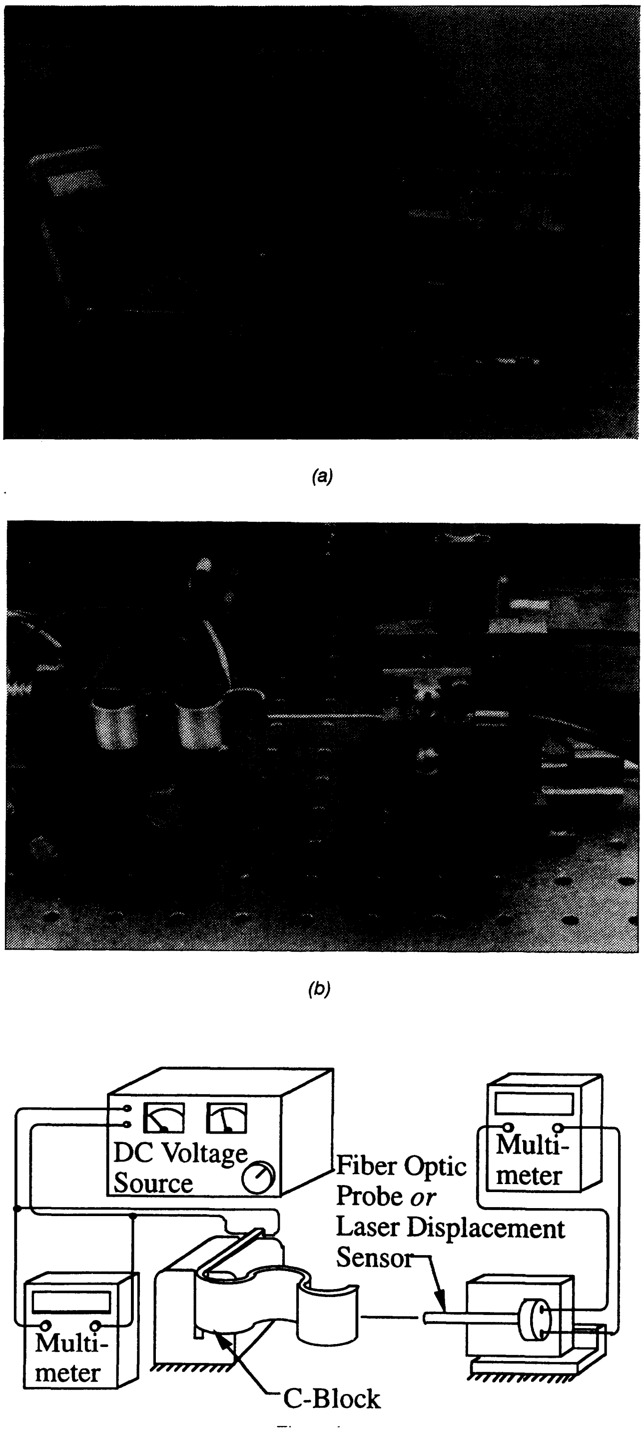

Figure 6. Experimental test setup for piezoceramic serial C-blocks. (a) The serial C-blocks were clamped in a vise and connected to a high-voltage DC power supply, monitored with a multimeter. (b) Tip displacement was measured with a fiber-optic displacement sensors. (c) A schematic diagram of the test equipment used.

ing the fiber optic displacement sensor. The voltage was decreased, again in regular intervals, back to zero volts, with displacement data taken at each interval. For the PZT-5H piezoceramic prototypes, the voltage was increased in intervals of 10 V to a maximum of 150 V, which corresponds to an electric field of 150 V/mm, or 37% of the breakdown voltage. For the PZT-8 piezoceramic prototypes and the polymeric prototypes, the voltage was increased to a maximum of 400 V in intervals of 25 V. For the PZT-8 prototype, this corresponds to an electric field of 526 V/mm, or 53% of the breakdown voltage; for the PVdF prototypes, this corresponds to an electric field of 7700 V/mm, or 26% of the maximum operating voltage.

Experimental Results

The results from this experimental procedure, along with the theoretical model [Equation (7)] are plotted in Figure 7 for piezoceramic case studies and in Figure 8 for the polymeric case studies. As Table 2 shows, the results from all experiments correlate very well with the theoretical model. The average difference between the theoretical model and experimental data is given for each prototype, and this difference as a percentage of the full-scale theoretical displacement is given as the error. The average error in all experiments was 3.55% with the maximum error for any prototype being 5.4%. Much of the difference between the theoretical model and experimental data is attributable to variations in the radius of the prototypes and the thickness of the epoxy bonding layer. The data obtained from the polymeric prototypes is more jagged due to uncertainties in measuring with the laser sensor the relatively large deflections generated. These uncertainties come primarily from the change in angular position of the surface of the C-block off which the sensor reads positional data. Some of the difference is also due to the presence of hysteresis, a common second-order phenomenon in piezoelectric materials, which was not accounted for in the theoretical derivation. The experimental data follow the linear form of the theoretical deflection-voltage model, showing that the deflection output from serial C-blocks is linear with voltage.

The case studies demonstrate the versatility of the C-block architecture with maximum deflections ranging from 8.8 microns to over 1200 microns. The case studies demonstrate that a wide deflection range is possible by varying the geometric, material, and configuration design parameters. For example, in the first baseline case study, the series of two PZT-5H C-blocks [Figure 7(a)] generate a total of 8.8 microns in deflection. This deflection output can be increased by changing the geometry of the prototype, as shown by the series of two PZT-8 C-blocks from the second case study [Figure 7(b)]. This prototype has a larger radius (19.9 mm versus 9.5 mm) and thinner cross-section (1.30 mm versus 1.89 mm) than the prototype of the first case study, which increases the deflection to 49.1 microns, substantially larger than the first case study.

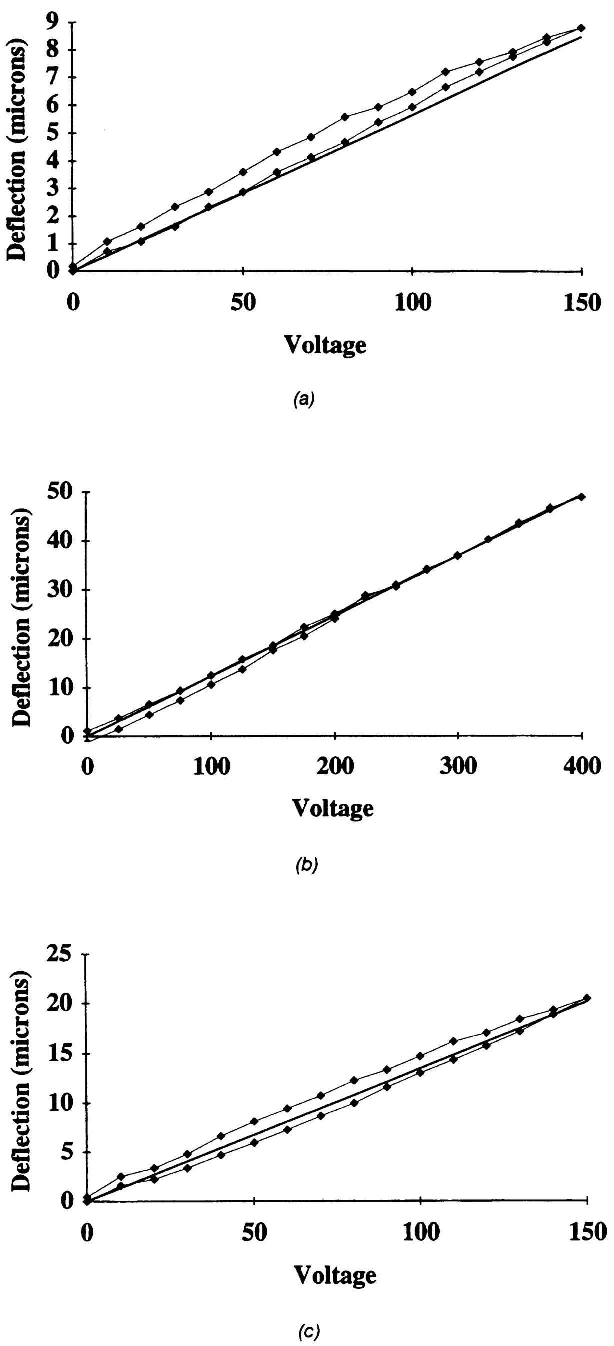

Figure 7. *Piezoceramic prototype deflection-voltage experimental results. The prototypes for the three piezoceramic case studies were experimentally tested to determine their deflection-voltage performance. The experimental results are graphed along with the deflection determined by the theoretical model [Equation (7)]. (a) Series of two PZT-5H C-blocks;* $R_{out} = 9.5$ *mm,* $t_p = 1.00$ *mm,* $t_s = 0.71$ *mm. (b) Series of two PZT-8 C-blocks;* $R_{out} = 15.9$ *mm,* $t_p = 0.76$ *mm,* $t_s = 0.41$ *mm. (c) Series of four PZT-5H C-blocks;* $R_{out} = 9.5$ *mm,* $t_p = 1.00$ *mm,* $t_s = 0.46$ *mm.*

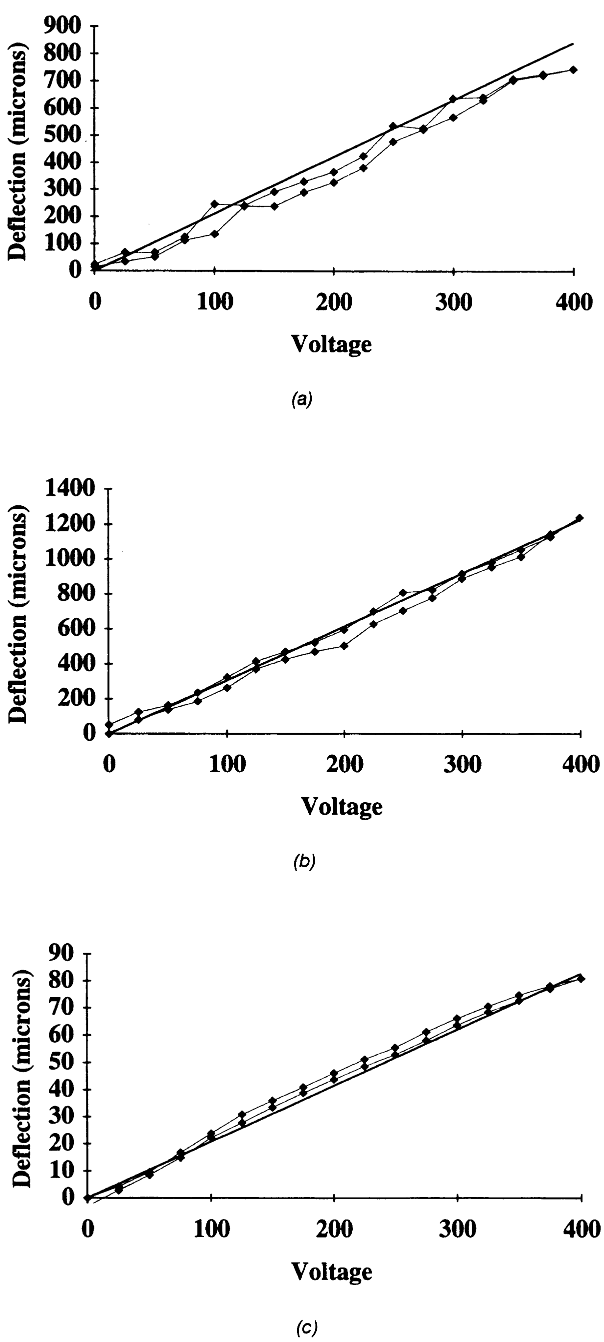

Figure 8. *Polymeric prototype deflection-voltage experimental results. The prototypes for the two polymeric piezoelectric case studies were experimentally tested to determine their deflection-voltage performance. The experimental results are graphed along with the deflection determined by the theoretical model [Equation (7)]. (a) Series of two PVdF C-blocks;* $R_{out} = 11.0$ *mm,* $t_p = 0.052$ *mm,* $t_s = 0.025$ *mm. (b) Series of three PVdF C-blocks;* $R_{out} = 10.8$ *mm,* $t_p = 0.052$ *mm,* $t_s = 0.025$ *mm. (c) Series of two PVdF C-blocks;* $R_{out} = 3.95$ *mm,* $t_p = 0.052$ *mm,* $t_s = 0.025$ *mm.*

Table 2. Differences between experimental data and theoretical model.

Case Study	Figure	Prototype Description	Maximum Displacement (microns)	Average Difference between Theory and Experiment (microns)	Percent Error
1	Figure 7(a)	(2) PZT-5H C-blocks	8.8	0.46	5.4%
2	Figure 7(b)	(2) PZT-8 C-blocks	49.1	0.69	1.4%
3	Figure 7(c)	(4) PZT-5H C-blocks	20.5	0.77	3.8%
4	Figure 8(a)	(2) PVdF C-blocks	841	45.3	5.4%
5	Figure 8(b)	(3) PVdF C-blocks	1222	29.3	2.4%
6	Figure 8(c)	(2) PVdF C-blocks	81	2.36	2.9%

The experimental data shown in Figures 7 and 8 were compared to the theoretical model [Equation (7)] for prototypes from all six case studies. The average difference between the experimental data and theoretical model is given, along with this error as a percentage of the full-scale theoretical displacement. The average overall error is 3.55%.

Another method for increasing the deflection is to change the material parameters; the fourth and fifth case studies show the effect of changing the material. The polymeric C-blocks in these case studies are roughly the same radius as the piezoceramic C-block in the first case study (11.0 mm and 10.8 mm versus 9.5 mm), but are considerably thinner than the piezoceramic C-blocks, and thus they deflect substantially farther than the 8.8 microns of the first case study. For example, the series of two polymeric C-blocks from the fourth case study gives 841 microns of deflection [Figure 8(a)], and the series of three polymeric C-blocks from the fifth case study gives 1222 microns of deflection [Figure 8(b)]. Analyzing the theoretical model helps clarify that the increase in deflection comes primarily from changes in the geometric rather than material parameters. Unfortunately, comparable thicknesses of polymeric and piezoceramic material were not available to test. Despite the substantially thinner cross-section and more compliant polymeric material, the error associated with the polymeric prototypes (Table 2) is approximately the same as the error associated with the piezoceramic prototypes.

One drawback to the larger deflection gained from the polymeric prototypes is that the deflection increase comes at the expense of force generation. Preliminary investigation shows that while the piezoceramic C-blocks in the first case study generates 4.5 Newtons of force, the polymeric prototypes of the fourth and fifth case studies generate only 7.3 milliNewtons of force, three orders of magnitude less than the first case study. This decrease in force is due to both the thinner cross-section of the polymeric C-block and reduced stiffness of the polymeric material. The series of two C-blocks in case study four and the series of three C-blocks in case study five both generate 7.3 milliNewtons of force. Thus, the force output is maintained as C-blocks are added in series. This is important since the actuator deflection can be increased without a corresponding decrease in force unlike straight bimorphs where the force decreases as the length is increased for greater deflection.

The force can also be increased by using a different lay-up. The sixth case study was investigated to determine the effect of a different lay-up on the deflection. This prototype was constructed using two layers of piezoelectric material with no substrate [Figure 8(c)]. This cross-sectional configuration can generate double the deflection and force of a unimorph because it has two active elements and no substrate. In the bimorph lay-up, the moment, M^P, is larger while the bending stiffness, D, is relatively unchanged. This also doubles the force output.

In addition to modifying the geometric and material parameters, the number of C-blocks in series can be used to effectively modify the deflection behavior. An example is shown by the series of four PZT-5H C-blocks from the third case study [Figure 7(c)]. The additional two C-blocks in series double the total deflection in comparison to the first case study, with the total deflection of this prototype being 20.5 microns. In this case, some additional deflection is gained due to the slightly thinner cross-section of the prototype. The fifth case study was used to test the deflection output from an odd number of C-blocks. The series of three polymeric C-blocks [Figure 8(b)] has a maximum displacement which is approximately 50% higher than the series of two, as predicted by the model; thus the simple theoretical model predicts the deflection produced from both odd and even C-block series. These case studies demonstrate that not only can C-block actuators be tailored using geometric parameters similar to other conventional technologies, but the deflection performance can also be simply tailored by utilizing architecture parameters such as the number of C-blocks in series.

CONCLUSION

This paper presented the theoretical and experimental investigation of the deflection performance of serial piezoelectric C-block actuator architectures. A model for the deflection-voltage performance of the serial C-block configuration was developed using Castigliano's second theorem, and the model was verified by fabricating and experimentally testing six prototypes fabricated from piezoceramic and polymeric piezoelectric material. These six case studies were used to explore the versatility of the architecture. The theoretical and experimental investigation demonstrated the following points:

- The theoretical model predicts the deflection-voltage behavior of a generic serial C-block actuator to within an average error of 3.55% of the full-scale theoretical deflection.
- The deflection of a serial C-block actuator is a linear addition of the deflections of each of the C-blocks in series and is a linear function of applied voltage.
- Maximum deflections from 8.8 microns to 1222 microns were achieved by varying geometric, material, and configuration parameters, demonstrating the versatility of the architecture.
- A variety of package sizes were physically realized with heights ranging from 8 mm to 32 mm.
- The deflection output of a serial C-block actuator can be increased in a predictable way by using individual C-blocks with larger radii and thinner cross-sections; however, this increase comes at the expense of force.
- The deflection output can be linearly increased without a corresponding decrease in force by combining C-blocks in series. This option is not available in many conventional actuators.
- Geometric changes have a stronger influence on deflection than material compliance. However, changes in material properties have a significant effect on force generation.

The fabrication, theoretical modeling, and experimental investigation of serial C-blocks demonstrate the versatility of the architecture. Since the deflection of a serial C-block is a linear addition of the deflections of the individual C-blocks in the series, increasing the deflection output of a series is a simple design task. This combination of properties makes the serial C-block easily tailorable to produce the required deflections and fit within volume-constrained applications.

ACKNOWLEDGEMENT

This material is based on work supported by the U.S. Army Research Office under grant number DAAH04-96-1-0186.

REFERENCES

Bamford, R., Kuo, C. P., Glaser, R., and Wada, B. K. 1995. "Long stroke precision PZT actuator," in *AIAA/ASME/ASCE/AHS/ASC Structures, Structural Dynamics, and Materials Conference—Collection of Technical Papers*, AIAA: 3278–3284.

Ben-Zeev, O., and Chopra, I. 1996. "Advances in the Development of an Intelligent Helicopter Rotor Employing Smart Trailing-Edge Flaps," *Smart Materials and Structures*, 5:11–25.

Brei, D., Ervin, J. D., and Moskalik, A. J. 1996. "Deflection-Voltage Performance of Asymmetrically Activated Piezoelectric C-Block Actuators," in *Smart Structures and Materials 1996: Smart Structures and Integrated Systems*, I. Chopra, Ed. SPIE Vol. 2717: 276–286.

Brei, D., and Moskalik, A. J. 1997. "Deflection Performance of a Bi-Directional Distributed Polymeric Piezoelectric Micromotor," *Journal of Microelectromechanical Systems*, 6:62–69.

Chandran, S., Kugel, V. D., and Cross, L. E. 1997. "CRESCENT: A Novel Piezoelectric Bending Actuator," in *Smart Structures and Materials 1997: Smart Structures and Integrated Systems*, M. E. Regelbrugge, Ed., Proc. SPIE 3041:461–469.

Damjanovic, D., and Newnham, R. E. 1992. "Electrostrictive and Piezoelectric Materials for Actuator Applications," *Journal of Intelligent Material Systems and Structures*, 3:190–208.

Dogan, A., Uchino, K., and Newnham, R. E. 1997. "Composite Piezoelectric Transducer with Truncated Conical Endcaps 'Cymbal,' " *IEEE Transactions on Ultrasonics, Ferroelectrics, and Frequency Control*, 44(3):597–605.

Face International. 1997. "THUNDER Actuators and Sensors," [brochure], available from Face International, 427 W. 35th St., Norfolk VA 23508.

Haertling, G. H. 1994. "Ultra-High-Displacement Actuator," *American Ceramic Society Bulletin*, 73(2):93–96.

Hall, S. R. and Prechtl, E. F. 1996. "Development of a Piezoelectric Servoflap for Helicopter Rotor Control," *Smart Materials and Structures*, 5:26–34.

Kugel, V. D., Chandran, S., and Cross, L. E. 1997. "Comparative Analysis of Piezoelectric Bending-Mode Actuators," in *Smart Structures and Materials 1997: Smart Materials Technologies*, W. C. Simmons, I. A. Aksay, and D. R. Huston, Eds., Proc SPIE 3040:70–80.

Moskalik, A. J., and Brei, D. 1996. "Force-Deflection Behavior of Individual Unimorph Piezoceramic C-Block Actuators," in *Proceedings of the ASME Aerospace Division*, J. C. I. Chang, J. Coulter, D. Brei, D. Martinez, W. Ng, and P. P. Friedmann, Eds., AD-Vol. 52:679–687.

Moskalik, A. J., and Brei, D. 1997a. "Frequency-Amplitude Response of Individual Polyvinylidene Fluoride Piezoelectric C-Block Actuators," in *Smart Structures and Materials 1997: Smart Structures and Integrated Systems*, M. E. Regelbrugge, Ed. SPIE Vol. 3041: 482–495.

Moskalik, A. J., and Brei, D. 1997b. "Quasi-Static Behavior of Individual C-Block Piezoelectric Actuators," *Journal of Intelligent Material Systems and Structures*, 8:571–587.

Onitsuka, K., Dogan, A., Tressler, J. F., Xu, Q., Yoshikawa, S., and Newnham, R. E.. 1995. "Metal-Ceramic Composite Transducer, The 'Moonie,' " *Journal of Intelligent Material Systems and Structures*, 6:447–455.

Paine, J. S. N., and Chaudhry, Z. 1996. "The Impact of Amplification on Efficiency and Energy Density of Induced Strain Actuators," in *Proceedings of the ASME Aerospace Division*, J. C. I. Chang, J. Coulter, D. Brei, D. Martinez, W. Ng, and P. P. Friedmann, Eds., AD-Vol. 52:511–516.

Samak, D. K., and Chopra, I. 1996. "Design of High Force, High Displacement Actuators for Helicopter Rotor Blade Control, " *Smart Materials and Structures*, 5:58–67.

Spencer, B. T., and Chopra, I. 1996. "Design and Testing of a Helicopter Trailing Edge Flap with Piezoelectric Stack Actuators," in *Smart Structures and Materials 1996: Smart Structures and Integrated Systems*, I. Chopra, Ed. SPIE Vol. 2717:120–131.